2014

A Semi-Empirical Prediction Model for the Discharge Line Temperature of Hermetic Compressors

David Myszka
University of Dayton, United States of America, dmyszka@udayton.edu

Chen Guan
University of Dayton, United States of America, magiccatgc12@gmail.com

Andrew Murray
University of Dayton, United States of America, amurray1@udayton.edu

Thomas Hodapp
Emerson Climate Technologies, Thomas.Hodapp@emerson.com

A semi-empirical prediction model for the discharge line temperature of hermetic compressors

David H. MYSZKA[1*], Chen GUAN[1], Andrew P. MURRAY[1], Thomas P. HODAPP[2]

[1] University of Dayton, Department of Mechanical and Aerospace Engineering, DIMLab
Dayton, OH, USA
dmyszka@udayton.edu, magiccatgc12@gmail.com, amurray1@udayton.edu

[2] Emerson Climate Technologies, Applied Mechanics
Sidney, OH, USA
thomas.hodapp@emerson.com

* Corresponding Author

ABSTRACT

Predicting the discharge line temperature (DLT) of air conditioning and refrigeration compressors is important to ensure sufficient lubricant properties and proper performance of components that are positioned in the exhaust stream. Understanding the DLT is also necessary for the design of waste heat recovery systems, which are of increasing interest. However, compressor performance information published by manufacturers does not typically include DLT values. Assumptions made in established thermodynamic models result in only modest correlation between predicted and observed DLT values. Numerous comprehensive DLT prediction models have been developed with excellent accuracy, but require many details of a particular compressor.

This paper presents an assessment of various thermodynamic DLT prediction methods that do not rely on individual compressor-specific parameters. Prediction methods considered include an entropy-based model, a polytropic model and an energy model. The energy model was expanded to include an empirical component to account for high-side heat transfer and exhibits an accuracy that significantly exceeds the other established methods. The model was evaluated for both traditional refrigeration and air-conditioning operating conditions and translates well to vapor-injected, economizer cycles. Lastly, a study was conducted to determine the robustness of the empirical component by analyzing the relationship between the accuracy of the model and the number of experimental points used to produce the model.

1. INTRODUCTION

A positive displacement compressor used in vapor-compression cooling systems increases the pressure of trapped refrigerant vapor by reducing its volume. Reducing the volume of a fixed amount of refrigerant vapor also increases its temperature, often referred to as the heat of compression (Hanlon, 2001). Predicting the temperature of the discharge line of an air-conditioning or refrigeration compressor is important to ensure that the components in the exhaust stream function properly. A primary concern with elevated temperatures is that refrigerant oils will start to break down or carbonize and may be insufficient to lubricate bearings and other moving components within the compressor (Stoecker, 2004).

Understanding the discharge line temperature (DLT) is also important in the design of waste heat recovery systems. In cooling systems, heat removed from a cooled chamber and heat generated by the compressor are stored in the refrigerant and rejected to the environment, representing waste heat. Waste heat recovery has long been studied for its potential as useful energy (Goldstic and Thumann, 1985; Kaushick and Singh, 1995). With greater emphasis being placed on energy conservation initiatives, engineers are more closely exploring strategies to utilize the waste heat recovery. Reclaiming this heat can be used to produce hot water (Ji et al., 2003), heat buildings (Sun and Li, 1999), and for drying clothing (Deng and Han, 2004).

Numerous models are published in the literature that simulate compressor performance. Many of these models include complete compressor operation including pressure profiles, valve behavior, instantaneous flow, leakage, component forces and lubrication (Suefuji et al., 1992; Chen et al., 2002). These models require a large number of parameters, many of which are only known by the manufacturer. Winandy et al. (2002) and Cabello et al. (2005) formulated simplified models to produce a good estimate of DLT and significantly reduce the number of compressor-specific parameters. However, these models still require the swept volume, built-in volume ratio, and separate heat transfer coefficients for different portions of the compressor.

For reliability purposes and to assess the heat energy available for reclamation, a prediction model of compressor discharge line temperatures that does not include compressor-specific parameters can be useful. This paper reviews alternative approaches and presents a semi-empirical model that produces good correlations with test data. The remainder of the paper is organized as follows. The vapor-compression cooling system is described in Section 2. Section 3 presents alternative DLT prediction models and provides an experimental evaluation of each. An empirically-based, adjusted energy approach is formulated in Section 4. Section 5 presents observations related to the sensitivity of the empirical model. The DLT prediction model is extended to economizer systems in Section 6.

2. COOLING SYSTEM DESCRIPTION

To identify the thermodynamic properties of refrigerant gas at different states within a refrigeration cycle, a schematic is shown in Fig. 1. The compressor draws a mass flow of cool, low pressure refrigerant gas at its inlet (state 2 in Fig. 1),

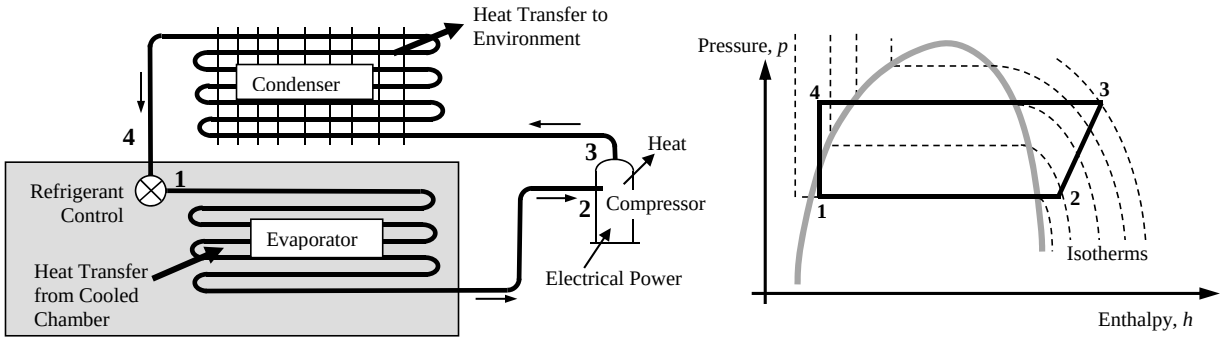

(a) Physical Components

(b) Cycle plot on a *p-h* grid

Figure 1: Schematic of a vapor compression cooling system.

and discharges hot, high pressure gas (state 3 in Fig. 1). The compressor is expected to operate at different cooling conditions signified by variations in the evaporator, condenser and compressor inlet conditions. ASHRAE (2010) specifies an operating condition with the following temperatures: the evaporator dew-point temperature T_e, the condenser dew-point temperature T_c, the temperature of the gas returning to the compressor T_2, the condenser liquid subcool temperature T_4 and ambient temperature T_∞.

2.1 Thermodynamic Analysis of the Cooling System

The compressor suction pressure p_2 is commonly assumed to be equal to the saturation pressure associated with the evaporator temperature T_e. That is, pressure losses in the suction line are considered negligible. Likewise, the compressor discharge pressure p_3 is assumed to be identical to the saturation pressure associated with the condenser temperature T_c.

An important principle of thermodynamics is the ***state postulate***, which asserts that the state of a compressible substance is completely defined by two independent properties (Sontag et al., 2008). That is, two given properties of a superheated refrigerant are sufficient to determine any other thermodynamic property. With given values of T_2 and p_2 at the compressor inlet, the suction density ρ_2, specific volume v_2, enthalpy h_2 and entropy s_2 can be determined

by using tables of the refrigerant thermodynamic properties (Dupont, 2011), refrigerant databases such as RefProp (Lemmon et al., 2013), or the Peng and Robinson (1976) equations of state .

2.2 Cooling System Performance Measures

The mass flow $\dot{m}$ is the average rate at which the compressor moves refrigerant through the cycle. Knowing compressor parameters, such as speed ω, displacement V_d, and volumetric efficiency η_v, the mass flow can be calculated as

$$\dot{m} = \eta_v \, \omega \, \rho_2 \, V_d. \tag{1}$$

The cooling capacity of the system $\dot{Q}$ at a specific operating condition is the rate at which heat is absorbed by the refrigerant from the chamber to be cooled. The enthalpy of the refrigerant exiting the condenser, h_4, is determined by the condenser pressure p_3 and the liquid subcool temperature T_4. No energy is exchanged within the refrigerant control valve, and $h_1 = h_4$. Capacity is calculated as the heat transfer rate across the evaporator,

$$\dot{Q} = \dot{m} \, (h_2 - h_1) \, . \tag{2}$$

The electrical power required to operate the compressor $\dot{W}$ is the rate at which work is performed to compress the refrigerant vapor, inefficiencies within the motor, friction, and flow losses. Defining η_c as the compressor efficiency, electrical power can be calculated as

$$\dot{W} = \frac{\dot{m}}{\eta_c} \int_{v_2}^{v_3} p \, dv. \tag{3}$$

Note that V_d, ω, the relationship between p and v, and compressor-specific losses must be known to apply Eqs. (1), (2), (3). Compressor rating is widely available and provides more accurate estimates of $\dot{m}$, $\dot{Q}$, and $\dot{W}$, as discussed in the following section.

2.3 Experimental Performance Data

Compressor manufacturers conventionally provide rating information across an operating map in accordance with ARI Standard 540 (2004). The compressor performance values are tabulated over a range of T_e and T_c. The tabular data is then represented by a ten-coefficient, third-order polynomial equation of the form

$$X = C_1 + C_2 T_e + C_3 T_c + C_4 T_e^2 + C_5 T_e T_c + C_6 T_c^2 + C_7 T_e^3 + C_8 T_e^2 T_c + C_9 T_e T_c^2 + C_{10} T_c^3. \tag{4}$$

where X can represent power input, mass flow rate, current or compressor unit efficiency. The rating coefficients C_i are determined by a regression and are provided by compressor manufacturers for engineers designing a system or components. Groll (2010) has reported succesfully using X to represent DLT values, however the corresponding coefficients are not consistently cataloged and are typically unavailable.

3. FUNDAMENTAL MODELS FOR DISCHARGE LINE TEMPERATURES

Three common models used to determine the DLT are evaluated in the following sections. The validity of the prediction models was assessed using 302 DLT measurements from various scroll compressors ranging from 2-ton to 15-ton, using various refrigerants (R22, R134a, R404A, R407A, R407C, R410A), evaporator temperatures ranging from -10 °F to 55 °F and condenser temperatures ranging from 70 °F to 140 °F.

3.1 Entropy Approach

As discussed in Sec. 2.1, the entropy at the compressor inlet s_2 and pressure at the exhaust p_3 can be generated from the operating point. Assuming an ideal, adiabatic compression process, the entropy of the exhaust gas will be the same as that of the inlet gas, $s_3 = s_2$. To account for inefficiencies, which would tend to increase exhaust entropy, an efficiency measure α was defined to model the increase. That is, $s_3 = \alpha \, s_2$. The exhaust entropy along with discharge pressure

(s_3, p_3) provides the two quantities necessary to use a refrigerant property database and determine T_3. Ignoring any heat transfer with the environment, the exhaust temperature T_3 is assumed equal to DLT. Using the 302 measurements, an iterative process was used to determine an efficiency measure of $\alpha = 1.0233$ that produced the lowest difference between predicted and measured DLT. The percent of measurements that fell within various error ranges is listed in Table 1. A plot of the correlation between predicted and measured DLT with $\pm 5\%$ bands is shown in Fig. 2a.

	Calculation Approach			
	Entropy	Polytropic	Energy Balance	Energy & Heat Loss
No. of Data-Based Parameters	1	2	1	3
Mean Prediction Error	0.00 °F	−0.046 °F	11.6 °F	0.00 °F
Prediction Std. Dev.	22.47 °F	19.06 °F	8.72 °F	3.30 °F
Prediction within ±5 °F	22.77 %	35.31%	19.33 %	92.41 %
Prediction within ±10 °F	39.60 %	61.72 %	51.00 %	98.35 %
Prediction within ±15 °F	53.14 %	80.20 %	69.67 %	99.34 %

Table 1: DLT prediction accuracy of alternative methods.

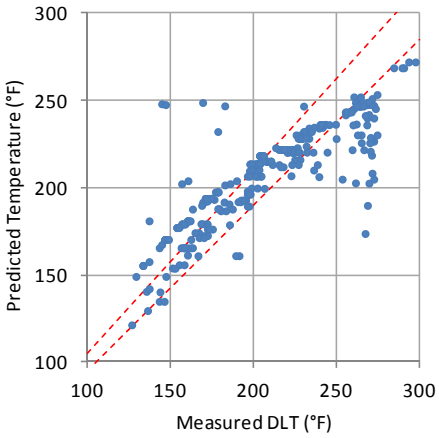

(a) Entropy approach

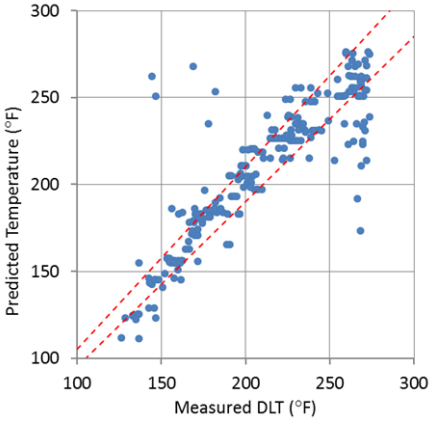

(b) Polytropic approach

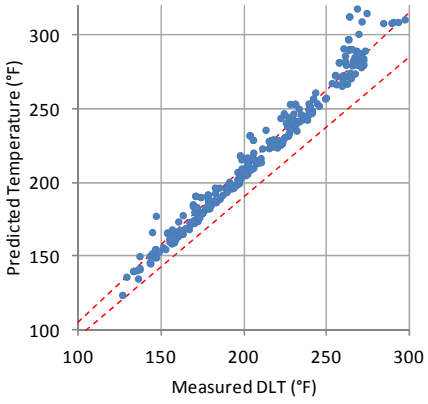

(c) Energy approach

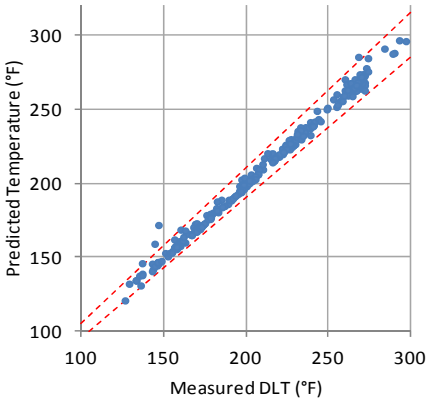

(d) Adjusted energy approach

Figure 2: Measured and predicted DLT correlation plots for the various approaches. The dashed lines represent a $\pm 5\%$ range.

3.2 Polytropic Compression Approach

A gas compression process is often considered as polytropic and follows the relationship

$$pv^{\gamma} = C \tag{5}$$

where γ is the polytropic exponent and C is a constant of proportionality. The value γ is experimentally determined, but for a given gas is often considered constant over a range of operating conditions (Lenz, 2002). For the compression process

$$\frac{p_3}{p_2} = \left(\frac{v_2}{v_3}\right)^{\gamma}. \tag{6}$$

The real gas equation of state is given as $pv = ZRT$, where R is a gas constant and Z is a compressibility factor. Substituting into Eq. (6) and rearranging,

$$T_3 = T_2 \frac{Z_2}{Z_3} \left(\frac{p_3}{p_2}\right)^{(\gamma-1)/\gamma}. \tag{7}$$

As in the previous approach, exhaust temperature T_3 is assumed equal to DLT. A regression was performed on each refrigerant to determine the values of γ and (Z_2/Z_3) that produced T_3 from Eq. (7) that produced the lowest difference between predicted and measured DLT. Resulting values obtained for γ are given in Table 2. The comprehensive prediction results are listed in Table 1 and a error plot with $\pm 5\%$ bands is shown in Fig. 2b.

Refregerant	R22	R134a	R404A	R407A	R407C	R410A
Z_2/Z_3	0.9855	1.0331	1.0131	0.9561	0.9525	0.9912
γ	1.2814	1.1447	1.1538	1.2173	1.2139	1.249

Table 2: Polytropic exponents for purpose of DLT prediction.

3.3 Energy Balance Approach

Energy flows into the compressor as electrical power $\dot{W}$ and with the inlet gas as $\dot{m}\, h_2$. As discussed in Sec. 2.1, the enthalpy at the compressor inlet h_2 and pressure at the exhaust p_3 can be generated from the operating point. Energy exits the compressor chamber with the exhaust gas as $\dot{m}\, h_3$. Rearranging this energy balance,

$$h_3 = \frac{\dot{W} + \dot{m}\, h_2}{\dot{m}}. \tag{8}$$

Since compressor coefficients for mass flow and electrical power are published in accordance with ARI Standard 540, $\dot{m}$ and $\dot{W}$ and are readily available. With h_3 and p_3 known, a refrigerant property database provides the exhaust temperature T_3. As with the other two approaches, heat transfer with the environment is ignored and DLT $= T_3$. The prediction results are listed in Table 1 and a error plot with $\pm 5\%$ bands is shown in Fig. 2c.

4. ADJUSTED ENERGY BALANCE APPROACH

Observing Fig. 2, the energy balance approach has the narrowest correlation band and warrants further investigation. Note from Table 1 that the energy approach has the lowest standard deviation, but the average estimated DLT is 11.6 °F higher than measured values. The DLT is lower than T_3 because of heat transfer from the hot, high-pressure side of the compressor to the environment. This high-side heat transfer $\dot{Q}_{ex}$ may be substantial as T_3 can be significantly above the ambient temperature T_{∞}. Expressing this high-side heat transfer energy balance gives,

$$\dot{m}\, h_3 - \dot{Q}_{ex} = \dot{m}\, h_{DL}. \tag{9}$$

where h_{DL} is the enthalpy of the refrigerant vapor as it enters the discharge line. Being a nearly constant pressure process, the specific heat c_p can be used to linearly relate the enthalpy difference to the temperature difference.

$$h_3 - h_{DL} = c_p \left(T_3 - \mathrm{DLT}\right). \tag{10}$$

Figure 3 illustrates the heat transfer from the hot, high side refrigerant through the compressor housing, which involves: a) forced convection from the refrigerant flow to the wall of the housing; b) conduction through the housing wall; c) free convection to the environment. The heat transfer across a series of conductive and convective barriers is expressed

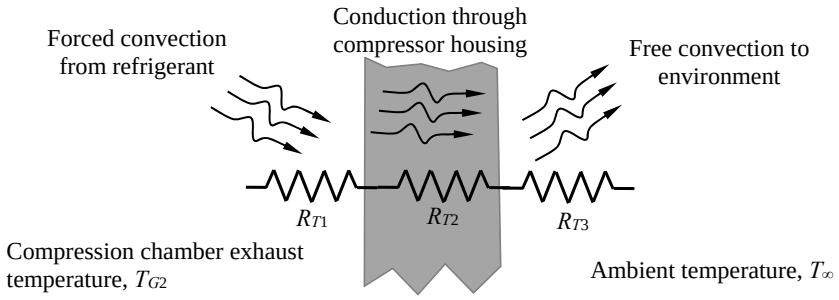

Figure 3: Heat transfer from the refrigerant exiting the compression chamber to environment.

in terms of the thermal resistance of each barrier R_{Ti} as

$$\dot{Q}_{ex} = \frac{T_3 - T_\infty}{\sum R_{Ti}}. \tag{11}$$

For both reciprocating compressors (Adair et al., 1972) and scroll compressors (Jang and Jeong, 2006), the thermal resistance of the forced convection portion of the heat transfer R_{T1} has been found to correlate with the Reynolds Number Re as established by Dittus and Boelter (1930),

$$R_{T1} = f(Re^{-0.8}). \tag{12}$$

The Reynolds Number is defined as $Re = \rho \bar{v} D/\mu$ where the D is diameter of the flow channel, $\bar{v}$ is the mean flow velocity, ρ is the refrigerant density and μ is the dynamic viscosity. Since $\dot{m} = \rho_2 \bar{v}(\pi D^2/4)$, the Reynolds number can be written as

$$Re = \frac{4\dot{m}}{\pi \mu D}. \tag{13}$$

While the shell size of hermetic compressors and viscosity of refrigerant is variable, the largest change among refrigeration compressor families and across the operating map occurs in the mass flow. Thus, the thermal resistance of heat flow from discharge gas to the shell is considered to be primarily dependent on the mass flow as

$$R_{T1} = f(\dot{m}^{-0.8}). \tag{14}$$

The thermal resistance of the compressor housing R_{T2} and the natural convection to the ambient R_{T3} are not dependent on the condition of the refrigerant flow, and consequently will have a low dependence on the compressor operating condition (T_e, T_c, T_2). While the diameter and shell thickness vary for different hermetic compressors, the percentage of variance is relatively minor. Thus, R_{T2} and R_{T3} will be considered constant. Combining Eqs.(10), (11), (13), (14), the temperature difference between exhaust and discharge line temperatures is expected to correlate to the mass flow as

$$T_3 - \mathrm{DLT} = A(T_3 - T_\infty)\frac{\dot{m}^{-0.8}}{c_p} + B, \tag{15}$$

where A and B are regression constants. Equation (15) was used with the 302 measurements previously discussed to provide regression values $A = 2.6564$ and $B = 1.4280$. This high-side heat transfer adjustment was applied to the energy balance discussed in the previous section. The prediction results for this adjusted energy approach are listed in Table 1 and an error plot with $\pm 5\%$ bands is shown in Fig. 2d. This alternative prediction strategy provides a modeling advantage over the other approaches.

5. OBSERVATIONS FROM THE DLT MODEL

A study was conducted to evaluate the number of measurement points required to construct an acceptable adjusted energy balance model. Of the 302 measurements, 100 random points were set aside to use as an evaluation data set. The remaining 202 measurements can be potentially used to determine the heat loss regression coefficients A and B. From these 202 measurements, $n = 15$ random points where used to construct the regression model of Eq. (15). This model was subsequently used to predict the DLT of the 100 evaluation points that were set aside. The regression was repeated, determining A and B with $n = 15$, 45, 90, and 180 random selected measurements. The prediction accuracy for various n measurements used to construct the regression model are provided in Table 3. Observed is that a larger sample size slightly improves accuracy at the $\pm 2\%$ level. However, the larger error bands do not show improvement and this accuracy limit is attributed to random measurement error. This study illustrates that Eq. (15) is an appropriate fit for the heat loss and relatively few measurements are required to perform the regression.

n	15	45	90	180
Prediction within $\pm 2\%$	57%	58%	60%	63%
Prediction within $\pm 5\%$	95%	96%	94%	95%
Prediction within $\pm 10\%$	100%	100%	99%	99%
Prediction within $\pm 15\%$	100%	100%	100%	100%

Table 3: DLT prediction accuracy with n points used to generating regression coefficients.

A second study applied the adjusted energy balance DLT prediction model to an externally generated data set. Winandy et al. (2002) formulated a simplified model that required only limited compressor-specific parameters. They provided 28 DLT measurements for an 8-ton hermetic compressor using R22, evaporator temperatures ranging from -5 °F to 55 °F and condenser temperatures ranging from 85 °F to 145 °F. Constants $A = 2.6564$ and $B = 1.4280$ (as determined in Sec. 4) were used in Eq. 15 and applied to that data set. An error plot with $\pm 5\%$ bands is shown in Fig. 4, illustrating good correlation.

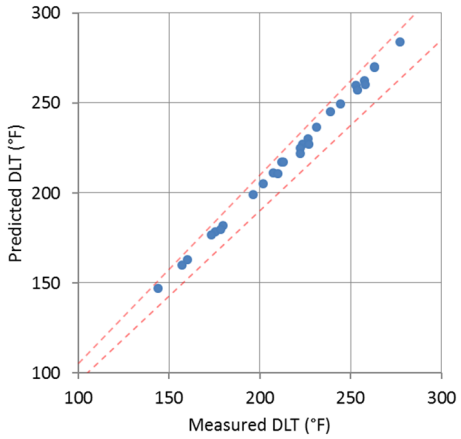

Figure 4: DLT correlation plot for the adjusted energy model applied to measurements presented in Winandy et al. (2002). The dashed lines represent a $\pm 5\%$ range.

6. ECONOMIZER, VAPOR-INJECTED CYCLE

The use of an economizer cycle, as shown in Fig. 5, can increase cooling capacity and efficiency of a cooling system. The DLT model was readily applied to the economizer cycle, accounting for the additional energy being introduced into the compressor with the injected refrigerant. The pressure of the vapor being injected into the compressor $p_7 \cong p_6$

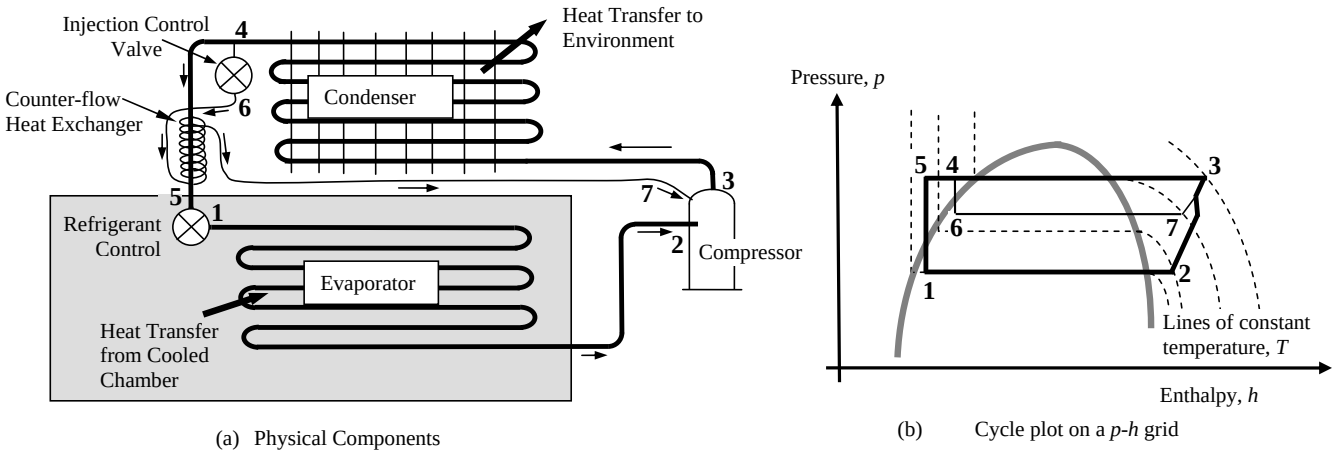

(a) Physical Components (b) Cycle plot on a *p*-*h* grid

Figure 5: Schematic of an economizer cooling system.

and the injected mass flow $\dot{m}_i$ become additional operating parameters. To differentiate between flows, the mass flow drawn through the compressor inlet is $\dot{m}_2$ and through the compressor outlet is $\dot{m}_3$. Thus, $\dot{m}_2 + \dot{m}_i = \dot{m}_3$.

The temperature of the refrigerant within the heat exchanger T_6 is taken as the saturation temperature corresponding with the injection vapor pressure p_6. The temperature of the injected refrigerant entering the compressor T_7 is typically 5 to 10 °F higher than the saturation temperature. For the purposes of this model, $T_7 = T_6 + 5$. Knowing the two properties of the injected refrigerant (T_7, p_7) the injection enthalpy h_7 can be determined from a refrigerant database. The energy balance of the suction plenum and compression chamber expressed in Eq. (8) must be modified to include the injected flow's enthalpy,

$$h_3 = \frac{\dot{W} + \dot{m}_2\, h_2 + \dot{m}_i\, h_7}{\dot{m}_3}. \tag{16}$$

For an economizer cycle, the energy approach with discharge plenum heat transfer adjustment can be used by replacing Eq. (8) with Eq. (16). This economizer prediction model was assessed using 219 DLT measurements from several different hermetic compressors ranging from 2-ton to 15-ton, using various refrigerants (R404A, R407A, R407C, R410A), evaporator temperatures ranging from -40 °F to 45 °F and condenser temperatures ranging from 50 °F to 140 °F. The error plot with $\pm 5\%$ bands is shown in Fig. 6.

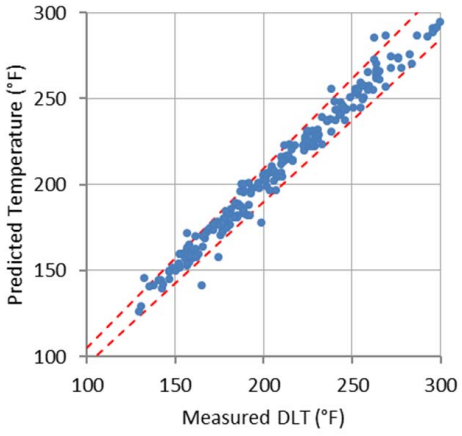

Figure 6: Measured and predicted DLT correlation plots for compressors operating in an economizer cycle. The dashed lines represent a $\pm 5\%$ range.

CONCLUSIONS

This paper assesses various DLT prediction methods that do not rely on compressor-specific parameters. Compared to entropy and polytropic models, an energy balance approach exhibited better correlation with experimental measurements. The energy balance approach was improved when an empirical heat loss term was added. A study was conducted to determine the relationship between the accuracy of the model and the number of experimental points used to produce the model. Lastly, the model was expanded to include vapor-injected, economizer cycles.

REFERENCES

Hanlon, P., 2001,*Compressor Handbook*, McGraw-Hill.

Stoecker, W., 2004, *Industrial Refrigeration Handbook*, Mc-Graw Hill.

Goldstick, R.J., Thumann, A., 1985, Principles of Waste Heat Recovery, *Association of Energy Engineers*, Atlanta, GA.

Kaushick , S. C., Singh, M., 1995, Feasibility and Design studies for heat recovery from a refrigeration system with a canopus heat exchanger, *Heat Recovery Systems & CHP*, vol.15, pp. 665-673.

Ji, J., Chow, T., Pei, G., Dong, J., He, W., 2003, Domestic Air-Conditioner and Integrated Water Heater for Subtropical Climate, *Applied Thermal Engineering*, vol. 23, pp. 581-592.

Sun, Z., Li, S., 1999, Analysis of Energy Reclamation of Air-Conditioning System, *Energy Conversion Technology*, vol 17, no. 6, pp. 26-28.

Deng, E., Han, H., 2004, An Experimental Study on Clothes Drying Using Rejected Heat with Split-type Residential Air Conditioners, *Applied Thermal Engineering*, vol. 24, pp. 2789-2800.

Suefuji, K., Shiibayashi, K., Tojo, K., 1992, Performance Analysis of Hermetic Scroll Compressors, *Proc. of the Int. Compressor Eng. Conf. at Purdue*, pp.75-84.

Chen, Y., Halm, N., Groll, E., Braun, J., 2002, Mathematical Modeling of Scroll Compressors - Part I: Compression process Modeling, *International Journal of Refrigeration*, vol 25, no. 6, pp. 731–750.

Winandy, E., Saavedra C., Lebrun, J., 2002, Experimental Analysis and Simplified Modeling of a Hermetic Scroll Refrigeration Compressor, *Applied Thermal Engineering*, vol. 22, no. 1, pp. 170-120.

Cabello, R., Navarro, J., Torrella, E., 2005, Simplified Steady-State Modeling of a Single State Vapor Compression Plant: Model and Verification, *Applied Thermal Engineering*, vol. 25, no. 4, pp. 1740-1752.

ASHRAE, 2010, *Methods of Testing for Rating the Performance of Positive Displacement Refrigerant Compressors and Condensing Units That Operate at Subcritical Temperatures Standard 23*, Atlanta, GA.

Sonntag, R., Bonrgnakke, C., Van Wylen, G., 2008, *Fundamentals of Classical Thermodynamics*, 7/e, John Wiley and Sons.

DuPont, 2011, *Thermodynamic Properties of Suva Refrigerants*, E. I. du Pont de Nemours and Company, Wilmington, DE.

Lemmon, E.W., Huber, M.L., McLinden, M.O., 2013, *NIST Standard Reference Database 23: Reference Fluid Thermodynamic and Transport Properties-REFPROP*, Version 9.1, National Institute of Standards and Technology, Standard Reference Data Program, Gaithersburg, TN.

Peng, D. Y., Robinson, D. B., 1976, A New Two-Constant Equation of State, *Industrial and Engineering Chemistry Fundamentals*, vol. 15, no. 1, pp. 59–64.

Lenz, J., 2002, Polytropic Exponents for Common Refrigerants, *Proc. of the Int. Compressor Eng. Conf. at Purdue*, Paper No. C9-3.

ANSI/AHRI, 2004, Standard for Performance Rating of Positive Displacement Refrigeration Compressors and Compressor Units, *Air-Conditioning, Heating, and Refrigeration: Standard 540*, Arlington, VA.

Groll, E., 2010, Overview of Compressor Technologies and their Analyses, *Short Course on Introduction to Compressors*, Ray W. Herrick Laboratories, Purdue University, West Lafayette, IN, July 10-11.

Adair, R. P., Qvale, E. B., Pearson, J. T., 1972, Instantaneous Heat Transfer to the Cylinder Wall in Reciprocating Compressors, *Proc. International Compressor Engineering Conference at Purdue*, pp. 521-526.

Jang, K., Jeong, S., 2006, Experimental Investigation on Conductive Heat Transfer Mechanism in a Scroll Compressor, *International Journal of Refrigeration*, vol. 29, no. 5, pp. 744-753.

Dittus, P. W., Boelter, L. M., 1930, Heat Transfer in Automotive Radiators of the Tube Type, *Univ. of Calif. Pub. Eng.*, Vol, 2, No. 13, pp. 443-461, 1930. (reprinted in *Int. Comm. Heat Transfer*, Vol. 12, pp. 3-22, 1985).